Gadolinium-DTPA in MR Imaging of Glioblastomas and Intracranial Metastases

Claus Claussen[1]
Michael Laniado[1]
Wolfgang Schörner[1]
Hans-Peter Niendorf[2]
Hanns-Joachim Weinmann[3]
Wiland Fiegler[1]
Roland Felix[1]

In 14 patients with the diagnosis of glioblastoma ($n = 7$) or intracranial metastases ($n = 7$), magnetic resonance (MR) imaging was performed using a variety of spin-echo (SE) pulse sequences before and after intravenous injection of 0.1 mmol gadolinium-DTPA (Gd-DTPA) per kilogram of body weight. In 10 patients, tumor tissue could not be adequately differentiated from perifocal edema on unenhanced scans with any of the applied pulse sequences. In four cases of intracranial metastases, poor differentiation between tumor and perifocal edema was possible in T2-weighted (SE 1600/70 and SE 1600/105) unenhanced scans. After administration of Gd-DTPA, tumor tissue showed marked contrast enhancement, and tumor delineation was consistently possible on SE 800/35 images. Tumor tissue could be differentiated from perifocal edema on SE 800/70 scans. Gd-DTPA is likely to increase the potential of MR imaging and refine the evaluation of glioblastomas and intracerebral metastases.

The advent of magnetic resonance (MR) imaging has broadened the spectrum of diagnostic methods in radiology. Clinical experience with MR imaging of the brain is accumulating rapidly. It has already been shown that the diagnostic potential of MR for lesions of the central nervous system is comparable to that of computed tomography (CT) [1–5]. In some cases, MR even seems to be diagnostically superior to CT (e.g., in posterior fossa tumors and brainstem tumors) [6–9].

The use of iodinated contrast agents makes contrast-enhanced CT scans superior to unenhanced MR images, particularly in demonstrating the margin between tumor and perifocal edema. Therefore, the development of specific contrast media for MR imaging was proposed [1–4, 7] and has become an attractive field of research.

Paramagnetic substances may be regarded as potent MR contrast agents if they enhance image contrast between magnetically similar but histologically dissimilar tissues by selectively decreasing proton relaxation times [10]. The gadolinium ion (Gd^{3+}), a rare-earth element, has favorable characteristics for this application because of its strong paramagnetic effect due to seven unpaired electrons [11]. When gadolinium is chelated with diethylenetriaminepentaacetic acid (DTPA), the stable complex Gd-DTPA [12–14] results, which is made highly water-soluble by forming a salt with N-methylglucamine. This new compound, gadolinium-DTPA–dimeglumine, has exhibited good contrast efficacy and good tolerance both in animals and in man [14–18].

We summarize our early experience with the use of Gd-DTPA for contrast-enhanced MR imaging in patients with glioblastomas and intracranial metastases. This report is part of an ongoing study to evaluate the diagnostic efficacy and tolerance of Gd-DTPA in MR imaging of intracranial tumors.

Materials and Methods

Fourteen patients with glioblastomas or intracranial metastases were selected for this

TABLE 1: **Summary of Patient Data**

Case No. (Age, Gender)	Diagnosis	Histology	Location
1 (41, M)	Glioblastoma (grade IV)	+	L occipital
2 (57, F)	Glioblastoma (grade IV)	+	L temporal
3 (56, F)	Glioblastoma (grade IV)	+	L parietooccipital
4 (52,M)	Glioblastoma	−	L temporal
5 (71,M)	Glioblastoma (grade IV)	+	L parietooccipital
6 (55,M)	Glioblastoma	−	R temporobasal
7 (67,M)	Glioblastoma (grade IV)	+	L frontal
8 (53,F)	Metastasis (unknown primary tumor)	+	L parietal
9 (71,M)	Metastasis (adenocarcinoma of colon)	−	R parietal
10 (50,M)	Metastasis (unknown primary tumor)	+	L parietal
11 (74,M)	Metastasis (bronchial Ca)	+	L occipitoparietal
12 (47,F)	Multiple metastases (bronchial Ca)	−	multiple
13 (65,M)	Metastasis (bronchial Ca)	+	L cerebellum
14 (51,F)	Multiple metastases (breast Ca)	−	multiple

Note.—Diagnoses were established by CT and confirmed in nine patients histologically (+ = confirmatory; − = not done). L = left; R = right; Ca = carcinoma.

TABLE 2: **Parameters of Spin-Echo Pulse Sequences**

Repetition Time (TR) (msec)	Echo Delay Time (TE) (msec)	Imaging Time (min)	No. of Slices
400	35	3.5	2
800	35	6.9	4
800	35 + 70	6.9	4
1600	35 + 70	13.8	8
1600	35 + 105	13.8	8

Note.—Two averages were acquired on each image.

study from patients examined by MR imaging before and after intravenous injection of Gd-DTPA. Written informed consent to participate in the study was obtained in each case. Patients were 41–74 years of age; five patients were female. Individual data are summarized in table 1.

Diagnoses were established in all patients by CT and confirmed in nine patients histologically. In those patients treated conservatively, the diagnoses were based on clinical and CT criteria. Three patients with intracranial metastases showed microscopic evidence of the primary tumor but not of the cerebral metastasis. Contrast-enhanced CT brain scans were available for each patient evaluated with MR imaging. All CT scans were obtained within 2 weeks of the MR studies. CT was performed on a Siemens Somatom 2, Somatom DR 2, or EMI 1010 head unit.

MR imaging was performed on a Siemens Magnetom superconducting whole-body scanner. This scanner generates a static magnetic field of 0.35 T and a corresponding radiofrequency of 15 MHz for hydrogen nuclei. The MR coil used for head imaging (diameter 25 cm) had a nominal spatial resolution of 1 mm in the section imaged. Transverse sections of the brain were obtained by multiple-slice technique. Section thickness was 10 mm with 10-mm spacing between adjacent sections. All images were produced using spin-echo (SE) pulse sequences and a two-dimensional Fourier transform image reconstruction technique. Various SE pulse sequences were used (table 2). Because of the large number of scans obtained in each patient, only two averages were acquired on a 256 × 256 matrix. The imaging time varied from 3.5 to 13.8 min according to the pulse

sequence used. Between two and eight slices were obtained on each examination. In any given case, three to six sequences were used to examine the region of interest. SE 400/35 (TR/TE) and 800/35 sequences were used in every case as the basic examination. To obtain images with T2 dependence, the initial images were supplemented by a long-TR SE technique (1600 msec) with a long TE (70 and 105 msec). Thus, the strongest intensity was recorded from tissues with high proton concentration and a long T2-relaxation time. In four patients, images were obtained using a double-echo technique with a repetition rate of 800 msec. A second echo at 70 msec, in addition to the one at 35 msec, was obtained before and after Gd-DTPA injection.

Gd-DTPA–dimeglumine (Schering AG, Berlin, West Germany) was made available to the investigators as an aqueous solution in a concentration of 0.5 mol/L. Gd-DTPA at a dose of 0.1 mmol/kg of body weight was injected at a rate of 10 ml/min into the antecubital vein after unenhanced MR images had been obtained. Depending on individual body weight, this dosage of contrast agent corresponds to an injected volume of 10–20 ml. To ensure complete administration of Gd-DTPA the catheter was flushed with 2 ml saline immediately after injection. The recording of contrast-enhanced scans began 5 min after administration of Gd-DTPA.

The MR images were reviewed independently by two observers. For all pulse sequences in both unenhanced and contrast-enhanced scans, information was grouped into several categories: tumor visualization, tumor delineation, visualization of edema, differentiation of tumor and edema, and degree of contrast enhancement after administration of Gd-DTPA (low, moderate, or intense).

Results

All seven patients with the diagnosis of glioblastoma had abnormal MR scans. Tumors were not directly visible on SE 400/35 and SE 800/35 scans, and lesions were identified mainly by mass effects and displacement of cerebral structures. Contrast between perifocal edema and brain generally was low and the edema was scarcely circumscribed (fig. 1A). Only one glioblastoma could be delineated on SE 800/35
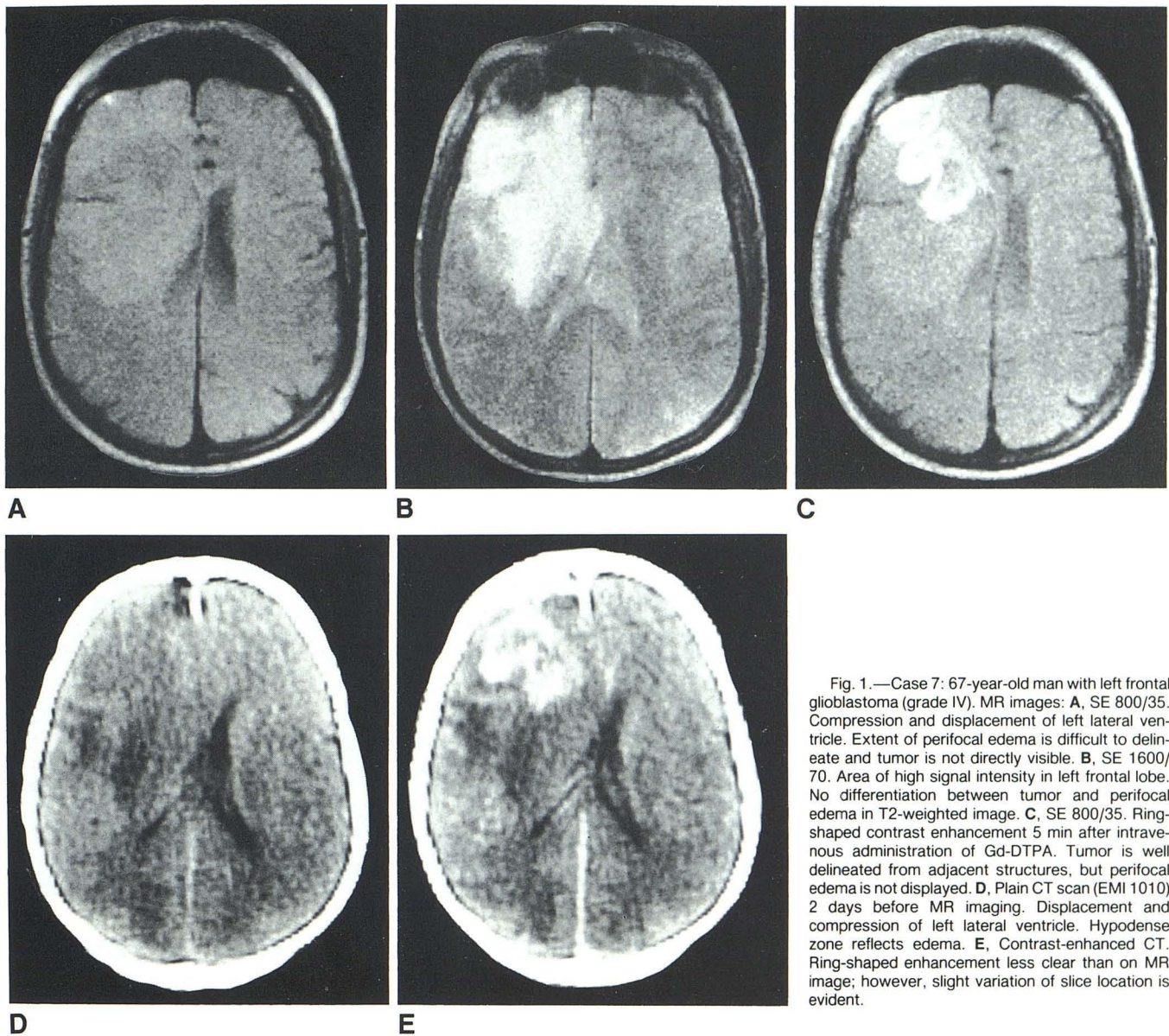
Fig. 1.—Case 7: 67-year-old man with left frontal glioblastoma (grade IV). MR images: **A**, SE 800/35. Compression and displacement of left lateral ventricle. Extent of perifocal edema is difficult to delineate and tumor is not directly visible. **B**, SE 1600/70. Area of high signal intensity in left frontal lobe. No differentiation between tumor and perifocal edema in T2-weighted image. **C**, SE 800/35. Ring-shaped contrast enhancement 5 min after intravenous administration of Gd-DTPA. Tumor is well delineated from adjacent structures, but perifocal edema is not displayed. **D**, Plain CT scan (EMI 1010) 2 days before MR imaging. Displacement and compression of left lateral ventricle. Hypodense zone reflects edema. **E**, Contrast-enhanced CT. Ring-shaped enhancement less clear than on MR image; however, slight variation of slice location is evident.

images, and the boundary between tumor and adjacent structures was poorly defined.

Low-density areas on CT had suggested the presence of perifocal edema in all cases of glioblastoma. These findings were consistently confirmed by T2-weighted images. The long-TR technique (1600 msec) showed high intensity, and focal tissue abnormalities on the 70-msec image, indicating prolonged T2 values (fig. 1B). As the echo delay time was increased in SE 1600/105 scans in four patients, contrast between edema and surrounding brain was generally increased, but this was balanced by a decrease in signal-to-noise (S/N) ratio with the result that lesions were not always better defined. On the other hand, differentiation between tumor and edema was not obtained either on SE 1600/70 or SE 1600/105 images. In three patients with glioblastoma examined by SE 800/35 as well as SE 800/70 pulse se-

quences, edema was shown more clearly on SE 800/70 images.

In the first image, obtained 5 min after contrast-medium injection, ring-shaped contrast enhancement in tumor tissue was visible in all glioblastomas, corresponding in shape and size with that seen on contrast-enhanced CT scans (figs. 1C and 1E). With SE 800/35 pulse sequences, contrast enhancement was apparent as an increase in signal intensity corresponding to a decrease in T1. The degree of enhancement was graded as intense in four patients and moderate in three. With contrast enhancement, the tumor tissue became distinguishable and was well delineated from adjacent structures. Perifocal edema was poorly visualized on enhanced SE 800/35 images. When images were acquired from the second echo (70 msec) in three patients with glioblastoma, less contrast enhancement was discerned after intravenous ad-
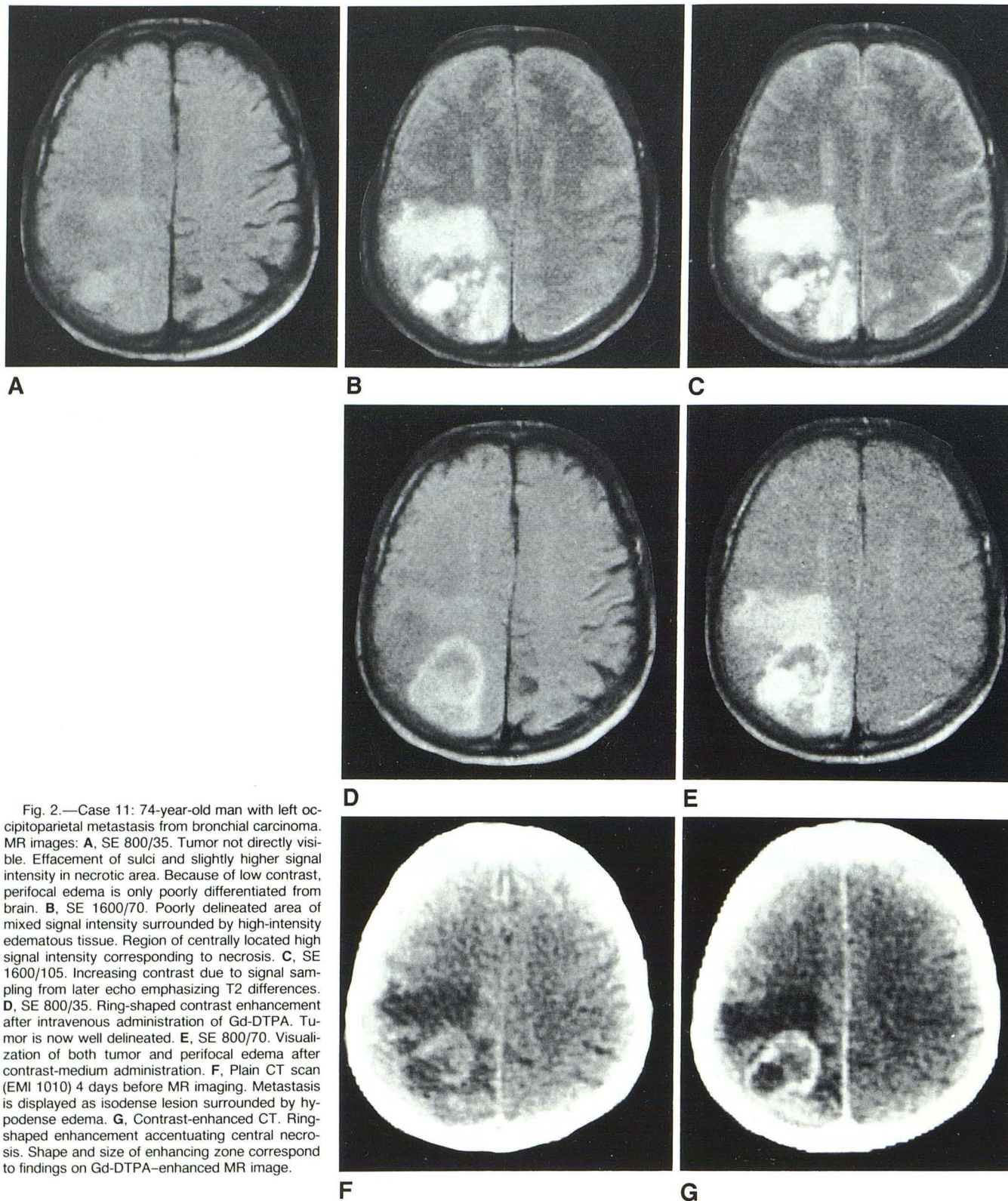
Fig. 2.—Case 11: 74-year-old man with left oc-cipitoparietal metastasis from bronchial carcinoma. MR images: **A**, SE 800/35. Tumor not directly visi-ble. Effacement of sulci and slightly higher signal intensity in necrotic area. Because of low contrast, perifocal edema is only poorly differentiated from brain. **B**, SE 1600/70. Poorly delineated area of mixed signal intensity surrounded by high-intensity edematous tissue. Region of centrally located high signal intensity corresponding to necrosis. **C**, SE 1600/105. Increasing contrast due to signal sam-pling from later echo emphasizing T2 differences. **D**, SE 800/35. Ring-shaped contrast enhancement after intravenous administration of Gd-DTPA. Tu-mor is now well delineated. **E**, SE 800/70. Visuali-zation of both tumor and perifocal edema after contrast-medium administration. **F**, Plain CT scan (EMI 1010) 4 days before MR imaging. Metastasis is displayed as isodense lesion surrounded by hy-podense edema. **G**, Contrast-enhanced CT. Ring-shaped enhancement accentuating central necro-sis. Shape and size of enhancing zone correspond to findings on Gd-DTPA–enhanced MR image.

ministration of Gd-DTPA than in SE 800/35 images. However, SE 800/70 images provided a high-intensity image of the perifocal edema while the enhanced tumor area also was well seen after contrast-medium administration.

The seven patients with single or multiple intracerebral metastases had positive evidence of space-occupying lesions on their MR scans. Before contrast-medium injection, SE 400/35 and SE 800/35 images consistently displayed indirect

tumor signs (mass effects and displacement) whereas direct visualization of tumor tissue was discerned in one patient only. As with gliobastomas, the perifocal edema was visualized by low contrast (fig. 2A). Perifocal edema was characterized on T2-weighted images by high signal intensity in all cases. In contrast to the findings in glioblastomas, T2-weighted pulse sequences (SE 1600/70 and SE 1600/105, respectively) provided differentiation between tumor and perifocal edema in four of seven cases, attributable to slightly lower signal intensities in tumor tissue as compared with perifocal edema (figs. 2B and 2C).

Five minutes after contrast-medium injection, the metastases were directly visible in SE 800/35 images in all seven patients owing to contrast enhancement (fig. 2D). The degree of enhancement was low in two patients, moderate in four, and intense in one. Accordingly, tumor delineation improved with higher contrast enhancement. As with glioblastomas, the shape and size of metastases on MR images after injection of Gd-DTPA corresponded to the findings on contrast-enhanced CT (fig. 2G).

SE 800/70 images were acquired in only one patient with intracerebral metastases. In accordance with the findings in glioblastomas, both tumor tissue and perifocal edema were visualized after contrast-medium administration (fig. 2E). However, the metastasis was only poorly delineated as compared with the delineation observed in contrast-enhanced SE 800/35 images.

Discussion

Intracerebral lesions that are accompanied by an increase in water content are generally characterized by a lengthening of both T1 and T2 relaxation times [3]. In most of the malignant intracerebral neoplasms this applies to the tumor tissue as well as to necrotic areas and perifocal edema [4, 6, 8, 19].

The most appropriate MR imaging techniques for the detection of tissues with prolonged relaxation times are T1- (e.g., SE 400/35) and T2-weighted pulse sequences (e.g., SE 1600/70) [2, 3, 19]. In spin-echo technique, prolonged T1 values tend to decrease signal intensity, whereas prolonged T2 values tend to increase signal intensity [3, 19]. Using a short repetition time in T1-weighted images, the nuclear magnetization of nuclei with long T1 times cannot recover completely between pulse intervals. Thus, signal strength arising from tissues with prolonged T1 values decreases. Therefore, these areas are displayed as darker than normal brain tissue [19]. However, our experience in MR imaging of brain tumors indicates that too-low contrast between normal and abnormal tissues is often displayed in T1-weighted SE images [20, 21].

In T2-weighted images (e.g., SE 1600/70) the long repetition rate enables nearly all spins to recover completely between imaging intervals, and the effects of differences in T1 relaxation are reduced [2, 3, 19]. The contrast is due to differences in T2 relaxation rates. Tissues with longer T2 times will be seen as relatively high-intensity regions. T2-weighted images are characterized by a wide contrast range but a lower S/N ratio than T1-weighted SE images. However,

it may be difficult to differentiate tumor tissue from surrounding edema even in heavily T2-weighted pulse sequences [1–4, 7, 8, 19–20]. In our study this applied to four of seven intracerebral metastases. In the case of glioblastomas, neither SE 1600/70 nor SE 1600/105 scans permitted differentiation between tumor and perifocal edema in any patient examined.

In the current study, this drawback of MR imaging was compensated for by using intravenous Gd-DTPA. This contrast agent was recently tested in a phase I study in healthy male volunteers. Good tolerance was observed as well as favorable pharmacokinetic properties [14–18, 22]. Subsequently, the first experience in patients with brain tumors demonstrated the contrast-enhancing properties of Gd-DTPA as being comparable to those of conventional contrast media in CT [18, 20, 21, 23, 24]. The hydrophylic gadolinium chelate was able to cross a damaged blood-brain barrier and influence relaxation times of areas of increased interstitial space, for the most part. However, edematous tissue is less affected because of the longer diffusion time of Gd-DTPA necessary to penetrate such areas.

Our current results impressively confirm the early findings. This is especially true in the diagnosis of glioblastomas examined before and after injection of Gd-DTPA. In all cases, a distinct contrast enhancement occurred in the ring-shaped tumor tissue typically seen in glioblastomas [25]. Although a slight differentiation between metastases and perifocal edema was achieved in four of seven cases on T2-weighted images, tumor delineation was definitely improved on SE 800/35 scans after contrast-medium administration. However, while the tumor tissue was greatly enhanced in this sequence, the edema was poorly or not at all displayed. By using a double-echo technique for enhancement, tumor tissue was visible in the first echo image whereas the second echo image at TE = 70 msec was most useful for the demonstration of both contrast-enhanced tumor tissue and perifocal edema. Our experience with contrast-enhanced SE 800/70 scans is limited, but results suggest that despite a decrease in S/N ratio, this sequence may be preferred for the visualization of tumor and edema after contrast-medium injection. No Gd-DTPA–related side effects have been observed so far.

The pattern of contrast enhancement in MR images largely corresponded to the findings on contrast-enhanced CT. The minor differences observable may reflect slight differences in slice location and in the inclination of the patient's head.

No biopsies were taken to give pathologic proof that the edge shown on the Gd-DTPA–enhanced images was in fact the edge of the tumor. However, autopsy studies have shown a remarkable correlation between the extent of contrast enhancement on CT and the extent of the tumor [26]. The pharmacokinetic properties are very similar to those of radiographic contrast agents [22]. Therefore, it is very likely that the zone of enhancement not only indicates a blood-brain-barrier disruption but also reflects the extent of invasion of the tumor tissue.

REFERENCES

1. Brant-Zawadzki M, Davis PL, Crooks LE, et al. NMR demonstration of cerebral abnormalities: comparison with CT. *AJNR* **1983**;4:117–124, *AJR* **1983**;140:847–854
2. Brant-Zawadzki M, Badami JP, Mills CM, et al. Primary intracranial tumor imaging: a comparison of magnetic resonance and CT. *Radiology* **1984**;150:435–440
3. Brant-Zawadzki M, Norman D, Newton TH, et al. Magnetic resonance of the brain: the optimal screening technique. *Radiology* **1984**;152:71–77
4. Bydder GM, Steiner RE, Young IR, et al. Clinical NMR imaging of the brain: 140 cases. *AJNR* **1982**;3:459–480, *AJR* **1982**;139:215–236
5. Zimmerman RA, Bilaniuk LT, Goldberg HI, et al. Cerebral NMR imaging: early results with a 0.12 T resistive system. *AJNR* **1984**;5:1–7, *AJR* **1983**;141:1187–1193
6. Bydder GM, Steiner RE, Thomas DJ, et al. Nuclear magnetic resonance imaging of the posterior fossa: 50 cases. *Clin Radiol* **1983**;34:173–188
7. McGinnis BD, Brady TJ, New PFJ, et al. Nuclear magnetic resonance (NMR) imaging of tumors in the posterior fossa. *J Comput Assist Tomogr* **1983**;7:575–584
8. Randell CP, Collins AG, Young IR, et al. Nuclear magnetic resonance imaging of posterior fossa tumors. *AJNR* **1983**;4:1027–1034, *AJR* **1983**;141:489–496
9. Young IR, Bydder GM, Hall AS, et al. The role of NMR imaging in the diagnosis of acoustic neuroma. *AJNR* **1983**;4:223–224
10. Brasch RC. Work in progress: methods of contrast enhancement for NMR imaging and potential applications. *Radiology* **1983**;147:781–788
11. Pople JA, Schneider WG, Bernstein HJ. *High-resolution nuclear magnetic resonance*. New York: McGraw-Hill, **1959**:209–217
12. Moeller T. Gmelin Handbuch der anorganischen Chemie: rare earth elements, part D1. Berlin/Heidelberg/New York: Springer-Verlag, **1980**
13. Grossman RJ, Wolf G, Biery D, et al. Gadolinium enhanced nuclear magnetic resonance images of experimental brain abscess. *J Comput Assist Tomogr* **1984**;8:204–207
14. Weinmann HJ, Brasch RC, Press WR, Wesbey GE. Characteristics of gadolinium-DTPA complex: a potential NMR contrast agent. *AJR* **1984**;142:619–624
15. Brasch RC, Weinmann HJ, Wesbey GE. Contrast-enhanced NMR imaging: animal studies using gadolinium-DTPA complex. *AJR* **1984**;142:625–630
16. Felix R, Laniado M, Claussen C, et al. Characterization of Gadolinium-DPTA. Basic properties and first clinical results. Presented at the 7th CARVAT, Rome, February **1980**
17. Laniado M, Weinmann HJ, Schörner W, et al. First use of Gadolinium-DTPA/dimeglumine in man. *Physiol Chem Phys Med NMR* **1984**;16:157–165
18. Schörner W, Felix R, Laniado M, et al. Prüfung des kernspintomographischen Kontrastmittels Gadolinium-DTPA am Menschen: Verträglichkeit, Kontrastbeeinflussung und erste klinische Ergebnisse. *ROFO* **1984**;140:493–500
19. Huk W, Heindel W, Deimling M, Stetter E. Nuclear magnetic resonance (NMR) tomography of the central nervous system: comparison of two imaging sequences. *J Comput Assist Tomogr* **1983**;7:468–475
20. Claussen C, Laniado M, Kazner E, et al. Application of contrast agents in CT and MRT: their potential in imaging of brain tumors. *Neuroradiology* **1985**;27:164–171
21. Schörner W, Felix R, Claussen C, et al. Kernspintomographische Diagnostik von Hirntumoren mit dem Kontrastmittel Gadolinium-DTPA. *ROFO* **1984**;141:511–516
22. Weinmann HJ, Laniado M, Mützel W. Pharmacokinetics of gadolinium-DTPA/dimeglumine after intravenous injection into healthy volunteers. *Physiol Chem Phys Med NMR* **1984**;16:167–172
23. Carr DH, Brown J, Bydder GM, et al. Gadolinium-DTPA as a contrast agent in MRI: initial clinical experience in 20 patients. *AJR* **1984**;143:215–224
24. Carr DH, Brown J, Bydder GM, et al. Clinical use of intravenous gadolinium-DTPA as a contrast agent in NMR imaging of cerebral tumours. *Lancet* **1984**:1:484–486
25. Kazner E, Wende S, Grumme T, et al. Computed tomography in intracranial tumors. Berlin/Heidelberg/New York: Springer-Verlag, **1982**
26. Wilske J. The anatomic correlate of the pathological cranial computerized tomogram. In: Lanksch W, Kazner E, eds. *Cranial computerized tomography*. Berlin: Springer-Verlag, **1976**:43–48